Title
Impact of Ethane and Propane Variation in Natural Gas on the Performance of a Model Gas Turbine Combustor

Authors
Flores, RM
McDonell, VG
Samuelsen, GS

Publication Date
2002

DOI
10.1115/gt2002-30080

Proceedings of
ASME TURBO EXPO 2002
June 3-6, 2002, Amsterdam, The Netherlands

GT-2002-30080

IMPACT OF ETHANE & PROPANE VARIATION IN NATURAL GAS ON THE PERFORMANCE OF A MODEL GAS TURBINE COMBUSTOR

R. M. Flores, V. G. McDonell, and G. S. Samuelsen[1]

UCI Combustion Laboratory
University of California
Irvine, CA 92697-3550
United States of America

ABSTRACT

In the area of stationary power generation, there exists a growing interest in understanding the role that gaseous fuel composition plays on the performance of natural gas-fired gas turbine systems. In this study, an atmospherically fired model gas turbine combustor with a fuel flexible fuel/air premixer is employed to investigate the impact of significant amounts of ethane and propane addition into a baseline natural gas fuel supply. The impacts of these various fuel compositions, in terms of the emissions of NO_X and CO, and the coupled impact of the degree of fuel/air mixing, are captured explicitly for the present system by means of a statistically oriented testing methodology. These explicit expressions are also compared to emissions maps that encompass and expand beyond the statistically based test matrix to verify the validity of the employed statistical approach.

MOTIVATION

In an effort to meet increasingly stringent emissions regulations, a number of researchers and manufacturers are now using lean-premixed gas turbine combustion as an alternative to other more traditional modes of gas turbine operation. Due to the complex nature of combustion systems, however, there remains much that is unknown about operating a combustion system lean; and there is even less known about operating lean and premixed. One unknown that is of growing concern is the effect that gaseous fuel variability may have on the performance of a lean-premixed natural gas-fired gas turbine system (e.g., Goy et al., 2001).

Recent work by Flores et al. (2001) revealed the degree to which the performance of a model gas turbine combustor was dependent upon the composition of the fuel. In that study, several different gaseous fuel blends were employed that included the addition of significant amounts of ethane or propane to the baseline fuel of natural gas. These fuels represented some of the extreme levels of ethane and/or propane that may be found within the natural gas supply of the United States (Liss et al., 1992).

The model combustor employed in Flores et al. (2001) was operated in a rapid mix mode of operation, and subtle differences in the fuel distribution—associated with differing momentum ratios for the various fuels—were found to affect the performance of the system. To extend the findings to a fuel/air premixer more representative of advanced practical mixers, the current study was undertaken. In addition, the present study utilizes experimental methods specifically directed at providing an explicit, quantitative relationship between the fuel composition and operation of the model combustor.

OBJECTIVES

The objectives of the current study are to (1) perform a series of statistically-based experiments examining the effects of fuel composition on the performance of a model gas turbine combustor, (2) to evaluate the effectiveness of the this statistical methodology with emissions and performance maps encompassing the model space, and (3) develop an explicit relationship between emissions performance and the combustor inlet fuel distribution and composition.

APPROACH

The approach taken is to develop and apply a modular Combustor Premixer with a flexible fuel injection system to provide control over the placement and distribution of the fuel within the combustion air stream. The fuel injection system is based on radial fuel jets that are located along the stem of the

1. corresponding author, gss@uci.edu
949 824-5950, 949 824-7423 FAX

Centerbody and the surrounding annulus wall of the Combustor Premixer. The ability to control the mixing and blending of the air/fuel mixture comprises a significant variable, along with the composition of the gaseous fuel blend, in the execution of a statistically based series of experiments.

The statistical experimentation is followed with the generation of emissions maps, as was done previously for a different system (Flores, et al., 2001). These maps are based upon the emissions of CO, NO_X, and the measured lean blowout (LBO) limits (ϕ_{LBO}) as measured for several specific fuel compositions, and will be generated as a function of radial fuel split and equivalence ratio. Additional insight concerning the effectiveness of this statistically based testing methodology is drawn from the measured distribution of the fuel, which is characterized at the inlet plane using an extractive probe.

EXPERIMENT

Test Facility

The test facility utilized provides a wide range of operating conditions and flow metering. The test stand is designed to operate at 1 atm with air inlet temperatures up to 800 K. The Combustor Premixer and Quartz Combustor Liner, shown schematically in Figure 1, are attached to a three dimensional traverse which allows the system to be moved as necessary about fixed diagnostic equipment and/or probes to map out points both within and at the exit plane of the Combustor.

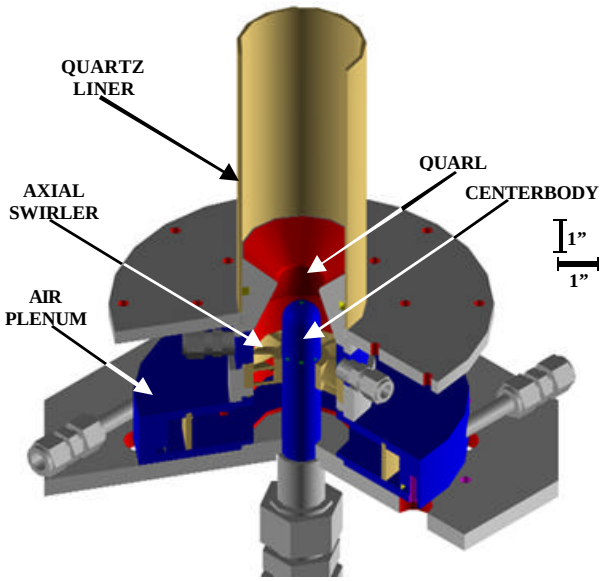

Figure 1: Relative Location of Centerbody & Combustion Premixer (Contraction & Exit Sampling Sections not Shown).

Combustor Premixer

A cross-sectional schematic of the Combustor Premixer from Figure 1 is provided in Figure 2 depicting the flow path of the combustion air entering the Combustor Premixer. Figure 3 shows the various fuel injection circuits available for the system, as well as their relative locations. The fuel injection system employs a total of ten gaseous mass flow controllers for monitoring and controlling the amount and placement of the blended fuel within the annulus of the Combustor Premixer. This provides for a multipoint approach to fuel and air mixing with the ability to control fuel flow splits between the various fuel injection circuits.

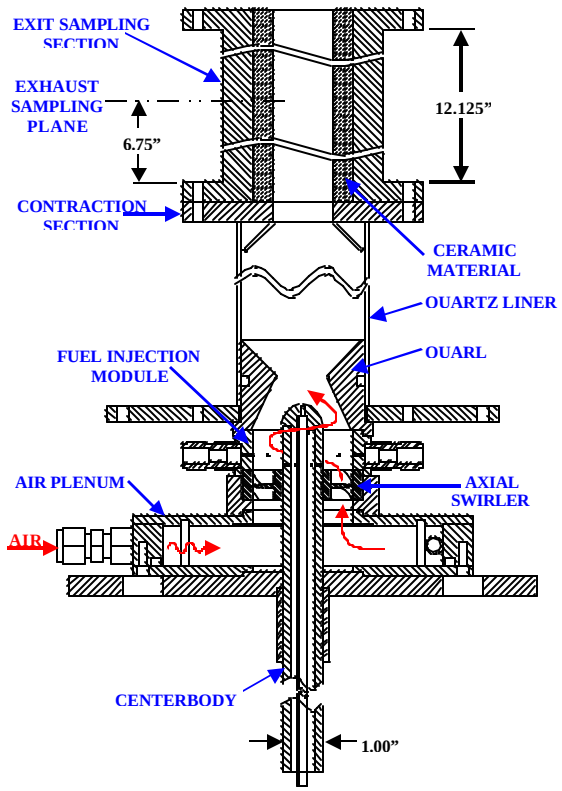

Figure 2: Cross Section & Air Flow Path of the System with an Axial Swirler & Exit Sampling Section.

With the present system, three independent fuel injection circuits are available. One option is to inject fuel radially from the Centerbody into the surrounding, swirling air stream. This Centerbody injection circuit, labeled "CB" in Figure 3, consists of eight equally spaced fuel holes located circumferentially along the stem of the Centerbody. The second fuel injection option is designed to inject the fuel radially from the surrounding annulus wall. This wall injection circuit, labeled "WJ" in Figure 3, also consists of eight equally spaced fuel holes in positions that are staggered with respect to the Centerbody injection holes. The final fuel injection option is to inject the fuel axially into the air stream. This axial injection circuit, labeled "PILOT" in Figure 3, consists of a single fuel injection hole located at the tip of the Centerbody.

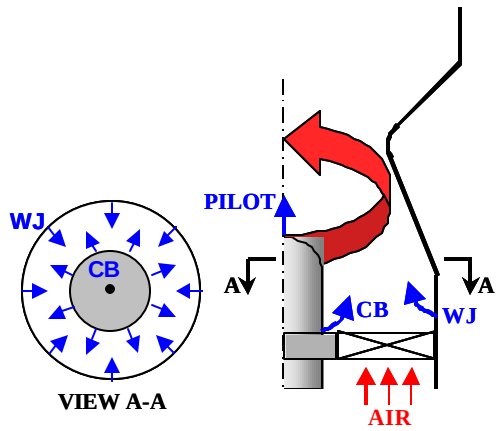

Figure 3: Relative Location and Number of the Fuel Injection Circuits.

By adjusting the distribution of the fuel between the radial and axial fuel injection circuits, the overall radial profile of the fuel distribution may be altered. This is demonstrated in Figure 4, where it is illustrated that, by varying the fuel from the Wall Injection Circuit to the Centerbody Injection Circuit, the fuel distribution can be weighted to either the centerline of the Combustor Premixer annulus or its wall. Likewise, additional fuel distribution weighting towards the centerline of the annulus may be achieved with the Pilot Injection Circuit. Figure 5 presents representative radial fuel distribution profiles with and without Pilot fuel for a given operating condition while illustrating that the composition of the fuel does not play a strong role in the overall curvature of the radial fuel distribution. This degree of fuel distribution control exceeds the level of control achieved previously in Flores et al. (2001).

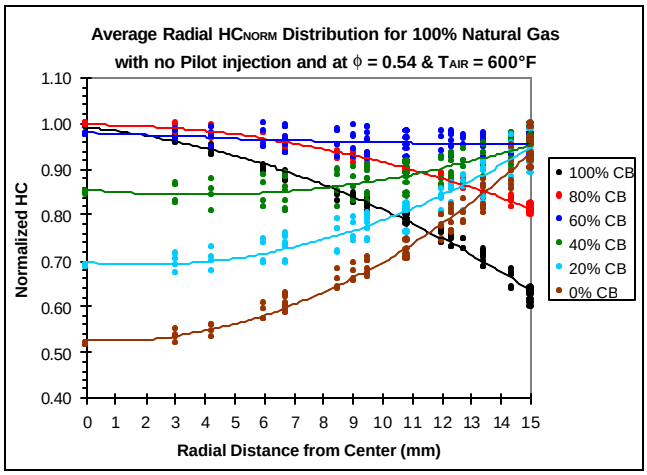

Figure 4: Typical Radial Profile of Fuel as a Function of Percent Centerbody

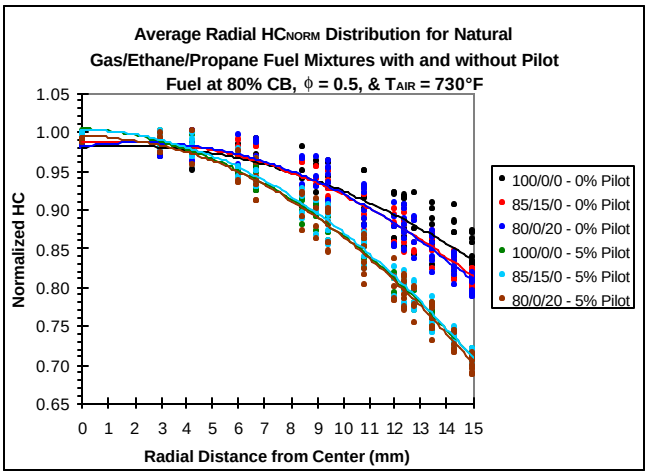

Figure 5: Representative Radial Fuel Distributions with and without Pilot Fuel

Additionally, the baseline configuration of the Combustor Premixer utilizes an eight vane, 45° axial swirler followed by a Fuel Injection Module (providing the fuel jets for the annulus wall), and a Quarl. The nominal firing rate for the system is 35 kW at 152.5 lbm/hr of air, though the fuel flow rates were varied to assess the performance of the system and applicability of the statistical results at different equivalence ratios. The air preheat temperature of the system was fixed at 660 K, which was achieved using an inline, non-vitiated, electrical air heater.

Diagnostics

Exhaust emissions of carbon monoxide (CO), carbon dioxide (CO_2), hydrocarbons (HC), oxygen (O_2), and nitrogen oxides (NO_x) were measured using Horiba Ltd. analyzers. These instruments are part of an integrated sampling and computer data acquisition system.

A 12.7 mm o.d. water-cooled, stainless steel bulk emissions probe is used to sample the exhaust emissions downstream of the exit plane of the combustor as shown in Figure 1. This probe is designed to take an integrated average measurement of the emissions over the diameter of the sampling plane via five area-weighted sampling ports. The water in the probe is heated to 325 K to protect the probe and quench the sample while avoiding condensation of water vapor inside the probe. The emissions are pumped through a Teflon line heated to 408 K to prevent water condensation, and the sample is then split into two streams. The NO_x stream goes through a converter to reduce any NO_2 to NO prior to the water drop out.

All of the emissions measurements from the analyzers are recorded using a digital data acquisition system. The data measurements from the analyzers are sampled and averaged over a 60 second period at a rate of 4 Hz. Error analysis and repeatability studies conducted on the fuel/air system and emission measurement equipment established an uncertainty of

±0.5 ppm (corrected to 15% O_2 by volume), for both CO and NO_X. Distributions of non-reacting fuel were mapped with a 12.7 mm o.d. stainless steel probe and a high range flame ionization detector (Horiba Model FIA-236-1) at the throat of the Quarl, immediately upstream of the Quartz Combustor Liner. All analyzers used had an accuracy of ±1% full scale.

Fuel Blending

The fuel blending system previously described in Flores et al. (2001) is also employed for the current study. As before, a subset of a comprehensive fuel blending system is utilized to blend streams of natural gas, ethane, and propane using a set of Brooks gaseous mass flow controllers. The blended gas stream pressurizes a fuel manifold and bypass line connected to a backpressure regulator. This fuel manifold supplies the necessary fuel at pressure to a second set of mass flow controllers that comprise the Fuel Injection Circuits of the Combustor Premixer. The entire process of monitoring and controlling the mass flow controllers is performed using a LabView based control program that allows the fuel composition and flow splits to be specified as desired. The overall accuracy of the blended fuel flow rate is ± 2%.

For the present study, the baseline fuel used is natural gas. A typical constituent composition of the available natural gas is summarized below in Table 1. The major constituent of the natural gas is methane, which is responsible for over 96% of the fuel's volume. Since a focus of this study is to examine the impact of significant increases in ethane and propane, the impact of the remaining minor constituents should be rendered negligible in comparison.

Table 1: Typical Natural Gas Composition.

n	Constituent		MF y(i) %
1	Methane	CH_4	96.975
2	Ethane	C_2H_6	0.982
3	Propane	C_3H_8	0.109
4	iso-Butane	C_4H_{10}	0.014
5	n-Butane	C_4H_{10}	0.015
6	iso-Pentane	C_5H_{12}	0.004
7	n-Pentane	C_5H_{12}	0.004
8	C6	C_6H_{14}	0.001
9	C7	C_7H_{16}	0.001
10	C8	C_8H_{18}	0.000
11	CO_2		1.574
12	O_2		0.000
13	N_2		0.322
		Totals	100.00

For the present study, three fuel compositions were considered for the emissions and performance maps to be compared with the statistical experiments. These three compositions represent the extremes in the fuel composition as described in the Motivation Section. Some of the associated properties are also summarized in Table 2.

Table 2: Gas Compositions Utilized.

Blend	Wobbe Index* MJ/m^3	S.G. relative to air	LHV MJ/m^3
Natural Gas	44.3	0.576	33.6
85% Natural Gas/ 15% Ethane	46.8	0.645	37.6
80% Natural Gas/ 20% Propane	50.5	0.765	44.2

** Wobbe Index = LHV / [SG]^{½} (Meier, et al., 1986)*

RESULTS

The results of the statistical experimentation are first presented and discussed. This is followed with a summary of the emissions maps that were generated. These emissions maps are then compared with the results of the statistical methodology to ascertain the validity of the statistical approach and to determine if the trends detected hold true under other conditions not directly considered in the statistical test matrix. Finally, a discussion of the relevant NO_X formation pathways is provided to ascertain the source of the NO_X generated during the course of this study.

Design of Experiments

The statistical approach applied to this study is based on a Design of Experiments (DoE) methodology, the fundamental aspects of which may be found in Box, Hunter and Hunter (1978). The DoE approach can be described as a systematic series of tests, in which purposeful changes are made to input factors of a process, so that one can observe and identify the reasons for the changes in the output responses. A benefit of this technique is its ability to avoid testing one factor at a time by incorporating randomization and multi-factorial experiments. By randomizing the sequence of experiments to be conducted, statistical and probability tools and techniques may be employed in the analysis of the results, including quantifying the amount of variability and uncertainty resulting from uncontrollable input factors while simultaneously identifying those parameters that have the most impact on the output of the system.

In general, there are two types of experiments that may be conducted under the DoE approach: Factorial and Mixture (See Cornell, 1990). While these two types of experiments may be fundamentally different, most of the same statistical tools applied to one experimental form may be applied to the other. The present study uses a combination of both types of experiments to create a single and more comprehensive experimental model. Such combinations of factorial/process components and mixture components are typically termed

"Crossed Experiments." In this case, the mixture components comprising the gaseous fuel blend are crossed with the process components of radial fuel split and percent pilot fuel injection at a fixed equivalence ratio and air preheat temperature.

Response Models

The final polynomial expressions for the responses (i.e., NO_X and CO) of the system are called the Response Models of the system. In the response models, each mixture component must always be represented since the total amount of a given mixture is always fixed. All other terms added to the response model—except those necessary to maintain hierarchy—were determined to have statistically significant (greater then 95-percent) impact upon the response of the system. Any terms added on a hierarchy basis was necessary to keep the model from becoming scale dependent.

The components and conditions used in the Crossed Experiment, and the terms that comprise Response Models are:

- Fixed Conditions
  - $\phi = 0.52$
  - $T_{AIR} = 730°F$
- Mixture Components
  - **A**: CH_4 = 80% - 100% (by volume)
  - **B**: C_2H_6 = 0% - 15% (by volume)
  - **C**: C_3H_8 = 0% - 20% (by volume)
- Process Components
  - **D**: % Pilot = 0% - 5%
  - **E**: % Centerbody = 100% - 40%

Using this combination of mixture and process components, a randomized test matrix consisting of only seventy-two experiments was generated. A sample of the test matrix is provided in Table 3. The total number of required measurements for this statistical approach is far less then would otherwise be required in a more traditional one-factor-at-a-time approach.

Table 3: Sample of Randomized Test Matrix.

A: CH_4	B: C_2H_6	C: C_3H_8	D: % Pilot	E: % CB
86.25	7.50	6.25	0.00	70
100.00	0.00	0.00	5.00	100
86.67	0.00	13.33	0.00	40
86.67	5.00	8.33	2.50	100
:	:	:	:	:
:	:	:	:	:
88.13	3.75	8.13	5.00	100
93.33	0.00	6.67	2.50	70
80.00	15.00	5.00	0.00	70

CO Response Model

The Response Model for the emissions of CO, in terms of actual factor units, is provided below in Equation 1. Note that the emissions of CO are measured in parts-per-million (ppm), and are corrected to 15% O_2 on a dry volume basis.

$$[CO]_{15\%} = 0.1029\mathbf{A} + 0.1216\mathbf{B} + 0.1511\mathbf{C} + 1.215\times10^{-4}\mathbf{AE} + 5.875\times10^{-4}\mathbf{BE} + 8.258\times10^{-4}\mathbf{CE}, \text{ (ppm)}$$

Equation 1

These results may also be depicted in graphical form as illustrated in Figure 6. Note that the results shown in Figure 6 are typical of other radial fuel splits, though the magnitude of the contour lines does change. Figure 6 indicates that the highest emissions of CO occur with the addition of propane with little contribution from ethane or methane.

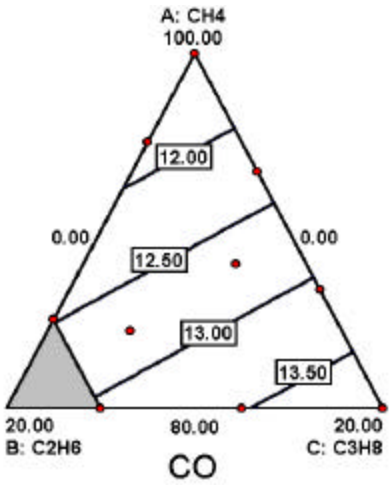

Figure 6: Mixture Space for CO at 100% Centerbody

A comparison of the predicted CO emissions from Equation 1 to the measured emissions is provided in Figure 7. This figure depicts the degree to which the Response Model can accurately predict the emissions of CO for a given set of conditions. The correlation coefficient (R-squared) of the model prediction compared to the measurements is 0.77. Note that the accuracy of the response model is independent of the reported accuracy of the individual measurements. The ability of the model to fit the measured data is dependent upon the judicious incorporation of components in the equation that are found to play the most significant role in impacting the response of interest, in this case CO.

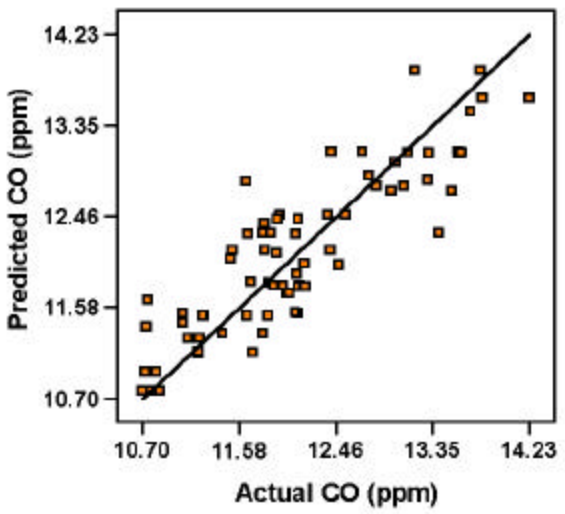

Figure 7: Predicted Versus Actual Values of CO

In order to ascertain the relative importance/impact of each term in affecting the final Response Model for CO, the Response Model is presented coded form in Equation 2.

$$[CO]_{15\%,CODED} = 11.14\mathbf{A} + 12.17\mathbf{B} + 13.09\mathbf{C} + 0.36\mathbf{AE} + 0.64\mathbf{BE} + 0.79\mathbf{CE}\ (\text{ppm})$$

Equation 2

The coded form of the Response Model, unlike the Response Model in terms of actual components, is based on assignment of the range of each component to a –1 (for minimum component value) to +1 (for maximum component value). This allows the relative impact of changes in the components on the emissions of CO to be ascertained by simply comparing the coefficients of the various terms. For example, the term **CE** has a coefficient that is about twice that of **AE**, implying that the combined impact on the CO from a change in the Percent Centerbody and Percent Propane is twice the impact seen for a similar change made to the Percent natural gas and Percent Centerbody. Additionally, all of the terms for the interactions in the coded form of the Response Model are positive, which implies that an increase in any of these Components will lead to an increase in the CO.

Further examination of the coded terms for Equation 2 leads to some interesting results. First, note that the coefficients for the three Mixture Components (**A**, **B**, & **C**) are substantially larger then any of the remaining terms. This implies that the emissions of CO—for the conditions under which this Crossed Experiment were conducted—are heavily influenced by the composition of the fuel. Increases in the radial fuel split (Percent Centerbody), for any fuel composition can also lead to an increase in the CO (given by the positive coefficients of the interacting terms), but the magnitude of increase is small relative to the overall magnitude of CO emissions. Additionally, there is no term showing an effect of the pilot fuel (**D**) in the coded Response Model. This means that the addition of pilot fuel, up to five-percent of the total fuel volume, had no statistically significant effect on the CO for the conditions considered.

NO_X Response Model

The Response Model obtained for the emissions of NO_X in terms of actual components and ppm, corrected to 15% O_2 on a dry volume basis, is provided below in Equation 3.

$$[NO_X]_{15\%} = 0.0677\mathbf{A} + 0.2548\mathbf{B} - 0.1506\mathbf{C} - 2.728\times10^{-3}\mathbf{AD} - 1.503\times10^{-3}\mathbf{AE} - 3.765\times10^{-3}\mathbf{BD} - 6.063\times10^{-3}\mathbf{BE} - 0.0193\mathbf{CD} + 7.333\times10^{-3}\mathbf{CE} + 1.248\times10^{-5}\mathbf{AE}^2 + 4.383\times10^{-5}\mathbf{BE}^2 - 4.991\times10^{-5}\mathbf{CE}^2 + 7.138\times10^{-5}\mathbf{ADE} + 9.078\times10^{-5}\mathbf{BDE} + 2.401\times10^{-4}\mathbf{CDE}\ (\text{ppm})$$

Equation 3

As with CO, these results may be depicted in graphical form, such as the examples shown in Figure 8 for 100% Centerbody (CB), and Figure 9 for 70% CB, both without Pilot fuel. It should also be noted that most of the results obtained without pilot fuel are similar to Figure 9 as the radial fuel split is varied from 100% CB. These figures indicate that the highest emissions of NO_X are obtained with the addition of propane, and that the role of the fuel composition on NO_X emissions also depends upon the radial distribution of the fuel. Both of these results are consistent with the findings of Flores et al. (2001). Figure 8 also indicates that the NO_X depends little on the fuel composition (i.e., the range in the contours is within experimental uncertainty). However, Figure 9 indicates that the fuel composition does play a role with 70% CB and that, specifically, propane is the primary driver. This interaction between the radial fuel distribution and the fuel composition is captured in the model shown in Equation 3.

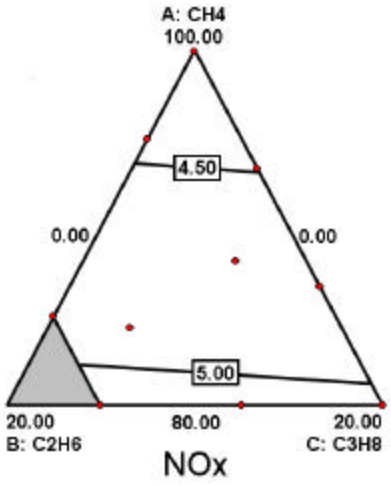

Figure 8: Mixture Space for NO_X at 100% Centerbody

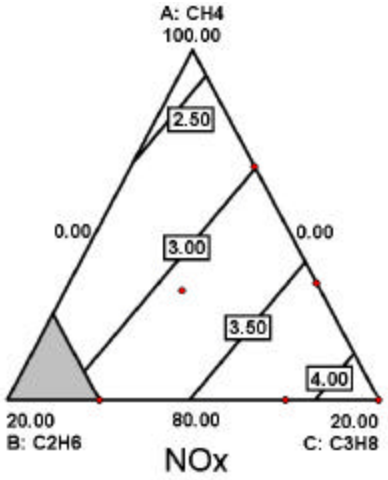

Figure 9: Mixture Space for NO_X at 70% Centerbody

A comparison of the predicted NO_X emissions from the Response Model to the actual NO_X emissions is provided in Figure 10. The data depicted in Figure 10 have a calculated R-squared value of 0.86.

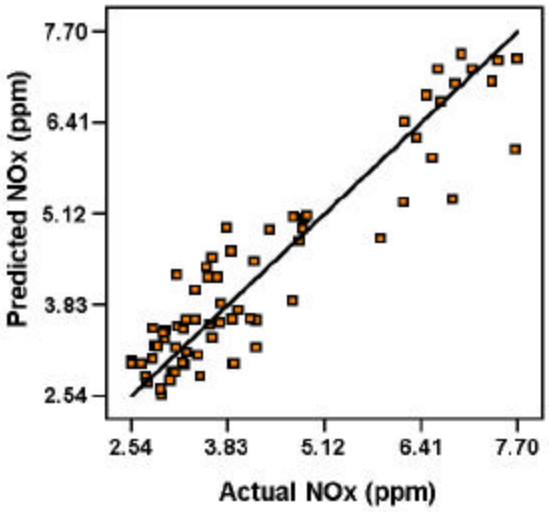

Figure 10: Predicted Versus Actual Values of NO_X

As with the CO, additional insight may be obtained from an examination of the coded from of the Response Model for NO_X. The NO_X Response Model in coded form is as follows:

$$[NO_X]_{15\%,CODED} = 2.93\mathbf{A} + 3.37\mathbf{B} + 4.58\mathbf{C} + 0.57\mathbf{AD} + 1.27\mathbf{AE} + 0.58\mathbf{BD} + 1.19\mathbf{BE} + 0.33\mathbf{CD} + 1.58\mathbf{CE} + 1.12\mathbf{AE}^2 + 1.69\mathbf{BE}^2 + 0.54\mathbf{ADE} + 0.56\mathbf{BDE} + 0.79\mathbf{CDE} \text{ (ppm)}$$

Equation 4

From Equation 4, the factors that play the most significant role in determining the level of NO_X emissions are the three gases used in the blend (i.e., the fuel composition). This is not to say that the mixture of the three gases is entirely dominant, but they have the most impact relative to the other terms. Also, propane again has the largest impact in affecting the level of NO_X emitted from the system, and not surprisingly, propane is followed by ethane and natural gas, respectively. This result is reflected by the coefficients of 4.58, 3.37, and 2.93 for propane, ethane, and natural gas, respectively.

Other interesting points may be made about the other terms that appear in the coded model, as well as a few points about terms that do not appear in the model. For instance, when comparing the coefficients for the terms AD and AE (the interaction between the methane ("A") and the components of % Pilot ("D") or % Centerbody ("E"), the Percent Centerbody plays a more important role then the Percent Pilot fuel injection, as characterized by AE's coefficient (1.27) versus AD's coefficient (0.57). This pattern repeats itself for ethane and propane. Just as telling is the fact that the percentage of the Centerbody has squared terms with significant coefficient values for all three fuel components, whereas the percentage of the Pilot has none. This result indicates a given composition of fuel will experience a significant rise in the level of NO_X emissions with an increase in the radial fuel split.

Lastly, the coded form of the NO_X model suggests that an interaction exists between the gaseous fuel composition and the addition of Percent Pilot and Percent Centerbody. This result makes sense in that increasing both the percentage of the Pilot and Centerbody leads to conditions where the largest amount of fuel is placed towards the center of the Combustor Premixer annulus (recall Figure 4 and Figure 5). This in turn leads to the highest "local" equivalence ratios achievable where Thermal NO_X may be generated at increased levels.

Emissions Maps

To examine the ability of the applied statistical methodology to accurately predict the trends of the present system for different fuel compositions, several emissions maps were generated. These emissions maps are for the extremes of fuel composition that were used in the Crossed experiments, were provided previously in Table 2, and were used in Flores et al. (2001) for a different type of injector. The emissions maps, with no Pilot fuel, are shown in Figure 11.

The emissions of NO_X and CO described on the maps in Figure 11 are corrected to 15% O_2, and are plotted as a function of equivalence ratio and radial fuel split (described in terms of the percentage of fuel injected radially outwards from the Centerbody). Also, the white regions on the lean side of each plot reflect regions beyond the LBO limits, where stable combustion could not be achieved. Note that the fuel split between the Centerbody and Wall injectors is of the remaining fuel *after* any pilot fuel is subtracted.

CO Emissions Maps

Recall that the statistical experimentation performed was for a fixed equivalence ratio of 0.52. However, several of the key observations made with respect to the CO appear to be valid for the CO emissions maps provided in Figure 11. One finding of the crossed experiments performed was that the emissions of CO were almost exclusively determined by the composition of the fuel, and that the radial fuel split had little impact on CO. A slight increase in the CO with an increase in the radial fuel split is noted, but that shift is small compared to the overall magnitude of the CO emissions as determined by the equivalence ratio and fuel composition. This is also illustrated in the CO plots of Figure 11 by the near vertical contour lines that only appear to shift to slightly higher levels of CO as the radial fuel split is increased and approaches a value of 100% Centerbody.

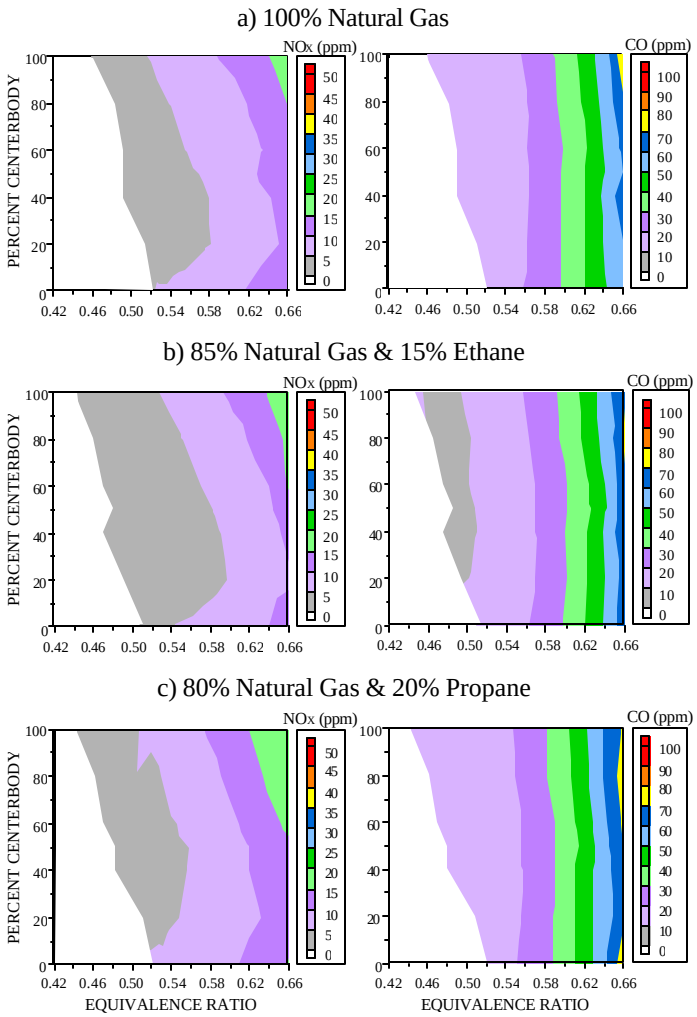

Figure 11: NO_X and CO Emissions Maps for Three Fuel Compositions without Pilot Injection

Likewise, the affect of the Pilot fuel on the emissions of CO is almost negligible, failing to rise above the experimental error (+/- 0.53 ppm) for these results. An emissions map for CO showing the impact of the Pilot fuel is therefore, not provided, given that there is little difference between such maps and their respective counterparts in Figure 11. This apparent lack of CO sensitivity to the overall fuel split is primarily due to the residence time of the fuel and air mixture in the combustion liner, and not the level of mixing generally achieved, since a similar result was obtained in Flores et al. (2001) with significantly poorer fuel and air mixing. Much of the CO that is produced, therefore, is given sufficient time to oxidize and form CO_2, and the overall fuel splits used in the crossed experiments (40-100% Centerbody and 0-5% Pilot fuel) does little to change this.

One inconsistency is observed between the maps and the Response Model. The CO Response Model indicates that the lowest emissions were for the fuel comprised of 100% natural gas, and generally highest with the addition of propane. The CO results of Figure 11 indicate, however, that it is actually the fuel composition with the significant levels of ethane that yield the lowest levels of CO. However, this difference may be attributed to the experimental error of the system as well as the scatter in the data comprising the CO Response Model (recall that Figure 7 had an R-squared value of 0.77).

NO_X Emissions Maps

One of the most interesting observations made via the NO_X Response Model was that the impact of the radial fuel split is second order in nature. Whether or not this observation holds up against the data represented in Figure 11 is not immediately obvious. As such, some of the NO_x data points from Figure 11a are graphed in Figure 12. Indeed, Figure 12 indicates that the emissions of NO_X increase rapidly with the radial fuel split as it approaches 100% Centerbody. Similar results to those provided in Figure 12 are also obtained for the other two fuel compositions mapped in Figure 11.

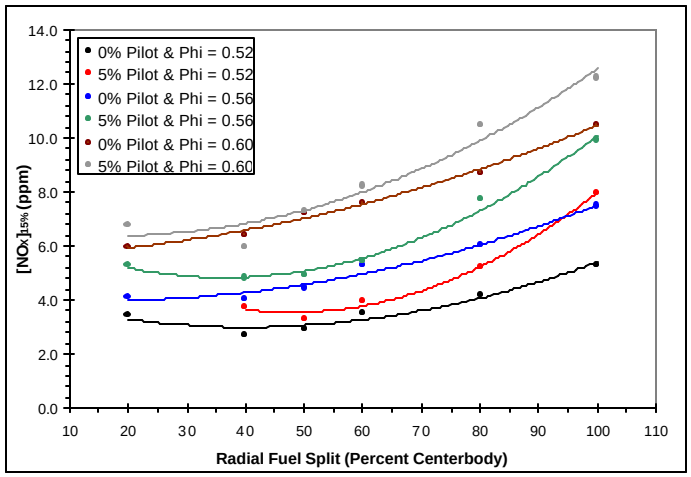

Figure 12: NO_X vs. Radial Fuel Split for 100% Natural Gas

It was previously mentioned that the NO_X Response Model indicated that the addition of propane would lead to the largest increase in the emissions of NO_X over the baseline fuel, followed by an increase in NO_X resulting from the addition of ethane. This observation, however, is not directly supported with the NO_X results provided in Figure 11, the addition of ethane led to lower emissions of NO_X then measured with the baseline fuel of 100% natural gas. A similar result was noted in the results of Flores et al. (2001) where some of the same fuel blends were examined on a different system at an air preheat temperature of 700 K.

The apparent discrepancy between the predicted behavior from Equation 3 and the detailed maps shown in Figure 11 is attributed to (1) the use of a single equivalence ratio for the development of the model, (2) the inability of the model to capture the subtle fuel effects revealed in the more detailed tests (i.e., R^2 of 0.86), and (3) the presence of experimental error associated with the measurements. Careful examination of Figure 9 does indicate that the Response Model predicts marginal increases in NO_X over the baseline fuel with significant amounts of ethane for at least some of the fuel split conditions.

Another parameter that is predicted to have an effect on the emissions of NO_X was the inclusion of fuel through the Pilot Circuit. The NO_X Response Model indicated that the addition of Pilot fuel would play a role in the formation of NO_X. For the cases with 20% propane, there is a significant increase in the formation of NO_X at radial fuel splits greater then 50% Centerbody (when compared for the case without Pilot fuel injection). For the other two fuel blends, the impact of the Pilot fuel is amplified as the radial fuel split increases above 60-70 Percent Centerbody (for the range of equivalence ratios plotted), supporting the **ADE**, **BDE**, and **CDE** terms listed in the coded form of the NO_X Response Model.

This result is due to the fact that increasing the radial fuel split directs additional fuel to the centerline of the Combustor Premixer annulus, where it begins to approximate a relatively well-mixed axial injector (recall Figure 4 and Figure 5). Add to this the effect of another five percent of the total volumetric flowrate in a manner that is not as well mixed as the radially injected fuel (but certainly not a diffusion type injector due to the mixing distance). Altogether, this allows the Pilot fuel stream to magnify/compound its apparent effect on the emissions of NO_X for the system.

Potential NO_X Formation Pathways

Given the significance and emphasis generally placed on the emissions of NO_X relative to the emissions of CO, a brief discussion as to the to likely sources of the NO_X emissions is warranted. Furthermore, given the relatively low equivalence ratios (and relatively low reaction temperatures that result) in Figure 11 and Figure 12, it is unlikely that the Thermal NO_X pathway is responsible for all of the measured NO_X, leading to a potentially significant contribution from other NO_X formation pathways. Moreover, the question arises about the specific role that fuel composition may have in the various non-thermal NO_X formation mechanisms.

In order to better understand the role of the fuel composition on the NO_X formed, and to gain insight into the potential for non-thermal NO_X pathways to contribute, some limited chemical kinetic calculations were conducted with a sensitivity analysis. Applying Chemkin's Senkin software package (Kee, 1999) and GRI Mech 3.0 to several selected conditions appears to suggest that it is likely that the NO_X generated was derived via the Nitrous Oxide (N_2O) Pathway in conjunction with the Thermal NO_X Pathway, with the N_2O Pathway likely responsible for a substantial portion (greater then 75%) of the NO_X measured. This is not surprising, however, when one considers that while Thermal NO_X may be present, it requires high reaction temperatures, typically above 1900K, to become dominant. Below this temperature, other NO_X pathways may play a significant role. Furthermore, the percentage and amount of NO_X formed from the N_2O pathway appears to increase with the addition of propane.

Another pathway, the Prompt NO_X pathway, likely contributes little to the overall emissions of NO_X from the system. Prompt NO_X, is unlikely to produce as much NO_X as the Thermal and N_2O Pathways. Prompt NO_X can continue to play a role at reaction temperatures below 1800K; however, in lean premixed systems, it has been indicated that Prompt NO_X is not a major source of NO_X until the equivalence ratio exceeds values greater then approximately 0.65 (Steele et al, 1998). The N_2O Pathway, on the other hand, has been found in other studies to play a significant role in the overall levels of NO_X emitted from lean premixed reactions with equivalence ratios less the 0.80 (Turns, 1996).

As such, a significant portion of NO_X measured and shown above must be a result of the N_2O Pathway. This is most likely for the cases with relatively well mixed fuel and air that create few, if any, "hot spots" that may accelerate the Thermal NO_X mechanism. However, the proportional contribution of the N_2O Pathway is reduced when compared to Thermal NO_X Pathway at conditions that are not well mixed, or have areas of locally high equivalence ratio (like those attained with high radial fuel splits and pilot fuel addition), where the production of Thermal NO_X may begin to significantly increase (See Figure 12). Note that Figure 4 and Figure 5 clearly indicate that while the overall equivalence ratios from Figure 11 may be low, the significant amount of fuel placed at the centerline of the Combustor Premixer annulus leads to areas of relatively high local equivalence ratio and temperature where Thermal NO_X becomes a stronger component of the overall NO_X emissions.

SUMMARY AND CONCLUSIONS

The results presented illustrate the potential for a Design of Experiments (DoE) testing methodology to provide a powerful tool to researchers conducting a variety of studies; in this case, a study focused in fuel compositional effects. The two general types of DoE methodologies, Factorial and Mixture, were

combined in a type of "hybrid" methodology called a "Crossed" methodology. This hybrid methodology sought to combine process and mixture components to examine the impact upon the selected responses of the system, which were the emissions of NO_X and CO. The effectiveness of the Crossed methodology was compared to additional data obtained and presented in the form of emissions maps for both NO_X and CO.

The results indicate that:

- The crossed model approach captures the majority of the emissions behavior noted in the emissions maps, and has generated an empirical expression that relates the emissions to both fuel composition and fuel distribution. The only significant discrepancy of this approach was its failure to capture the subtle reduction in emissions obtained with the addition of significant amounts of ethane.
- CO formation is dominated by the fuel composition with higher hydrocarbons leading to higher CO levels. The fuel distribution and operation of the pilot has little influence on the CO levels in this system.
- NO_X formation in the present system is dependent upon the fuel composition, but also exhibits subtle dependencies upon the fuel distribution and the use of the pilot. The crossed model generates an expression that captures the coupling between the fuel distribution and the composition.
- The composition of the fuel had a negligible impact upon the curvature of the radial fuel distribution profile entering the combustor.
- The emissions of CO were noted to be relatively insensitive to the radial fuel split for both the present system as well as the system previously used in Flores et al. (2001), which achieved relatively poor fuel and air mixing.
- Limited kinetic calculations with a sensitivity analysis appears to suggest that the Nitrous Oxide Pathway predominantly responsible for the measured emissions of NO_X.

ACKNOWLEDGEMENTS

The authors acknowledge the support of the US Department of Energy Advance Turbine Systems program and the South Carolina Institute for Energy Studies (SCIES). The contributions of Mr. Junhua Chen, Dr. Jack Brouwer, and Mr. Steve Hill are gratefully appreciated.

REFERENCES

Box, G. E. P, Hunter, W. G., and Hunter, J. S., Statistics for Experiments, John Wiley & Sons, Inc., New York 1978.

Cornell, J.A., Experiments with Mixtures: Designs, Models, and the Analysis of Mixture Data, 2nd ed., John Wiley & Sons, Inc., New York 1990.

Flores, R.M., Miyasato, M.M., McDonell, V.G., and Samuelsen, G.S. (2001). Response of a Model Gas Turbine Combustor to Variation in Gaseous Fuel Composition, J. Engr. Gas Turbines and Power, Vol. 123, No. 4, pp. 824-831.

Kee, R.J. et al. (1999). Chemkin Collection, Release 3.5, Reaction Design, Inc., San Diego, CA.

Goy, C.J., Moran, A.J., and Thomas, G..O. (2001). Autoignition Characteristics of Gaseous Fuels and Representative Gas Turbine Conditions. Paper 2001-GT-0051, presented at the TURBOEXPO 2001, 4-7 June 2001, New Orleans, LA.

Liss, W.E., Thrasher, W.H., Steinmetz, G.F., Chowdiah, P, and Attari, A. Variability of Natural Gas Composition in Select Major Metropolitan Areas of the United States, GRI-92/0123 March 1992.

Meier, J.G., Hung, W.S.Y., and Sood V.M. (1999). Development and Application of Industrial Gas Turbines for Medium-BTU Gaseous Fuels, J. Engr. Gas Turbine and Power, Vol. 108, pp. 182-190.

Steele, R. C., Tonouchi, J. H., Nicol, D. G., Horning, D. C., Malte, P. C., and Pratt D. T. (1998). Characterization of NO_X, N_2O, and CO for Lean-Premixed Combustion in a High-Pressure Jet-Stirred Reactor, J. Engr. Gas Turbines and Power, Vol. 120. Pages 303-10.

Turns, S.R., An Introduction to Combustion: Concepts and Applications, McGraw – Hill, New York 1996.